



**IEEE Xplore®**  
RELEASE 1.8

Welcome  
United States Patent and Trademark Office

**IEEE Xplore®**  
1 Million Documents  
1 Million Users

[Help](#) [FAQ](#) [Terms](#) [IEEE Peer Review](#)

**Quick Links**

» **ABSTRACT PLUS**

Welcome to IEEE Xplore®

- ☐ Home
- ☐ What Can I Access?
- ☐ Log-out

Search Results [PDF FULL-TEXT 132 KB] [NEXT](#) [DOWNLOAD CITATION](#)



Tables of Contents

- ☐ Journals & Magazines
- ☐ Conference Proceedings
- ☐ Standards

Search

- ☐ By Author
- ☐ Basic
- ☐ Advanced
- ☐ CrossRef

Member Services

- ☐ Join IEEE
- ☐ Establish IEEE Web Account
- ☐ Access the IEEE Member Digital Library

IEEE Enterprise

- ☐ Access the IEEE Enterprise File Cabinet

Print Format

## The design methods of current-mode nth-order filters

Wang Xiufang Gao Bingkun

Daqing Pet. Inst., China;

*This paper appears in: Intelligent Control and Automation, 2000. Proceedings of the 3rd World Congress on*

Meeting Date: 06/28/2000 - 07/02/2000

Publication Date: 28 June-2 July 2000

Location: Hefei China

On page(s): 2570 - 2571 vol.4

Volume: 4

Reference Cited: 2

Number of Pages: 5 vol. 3828

Inspec Accession Number: 6770322

### Abstract:

The design methods of nth-order filters by means of current conveyor (CC) are studied, the filter circuits using second-generation CC and multi-output CC (MOCC) are compared and the merit and defect of two design methods are analyzed. The result states clearly that an nth-order filter designed by means of MOCC has a small mount component and simple structure and has good potential for use in information processing

### Index Terms:

active filters current conveyors current-mode circuits network synthesis CCII current conveyor current-mode high-order filter design filter circuits multi-output CC second-generation CC

### Documents that cite this document

There are no citing documents available in IEEE Xplore at this time.

Search Results [PDF FULL-TEXT 132 KB] [NEXT](#) [DOWNLOAD CITATION](#)

# THE DESIGN METHODS OF CURRENT-MODE NTH-ORDER FILTERS

Wang, Xiufang Gao, Bingkun  
Daqing Petroleum Institute And 151400

**Abstract:** The design methods of nth-order filters by means of CC are studied, the filter circuits using CCII and MOCC are compared, and the merit and defect of two design methods are analyzed. The result states clearly that nth-order filter by means of MOCC has a small mount component and simple structure and has a bright future in the system of information processing.

**Key words:** Current conveyor, Active filters, Nth-order filters

## 电流模式 n 阶滤波器的设计方法

王秀芳 高丙坤

(大庆石油学院自控系 安达 151400)

**摘 要:** 研究用 CC 实现 n 阶滤波器的设计方法, 通过比较用 CCII 和 MOCC 实现的滤波器电路, 分析了两种不同设计方法的优劣。分析结果表明, 用 MOCC 综合的 n 阶滤波器含有较少的元件, 电路结构简单, 在信息处理系统中有较好的使用前景。

**关键词:** 电流传送器, 有源滤波器, n 阶滤波器

### 1. 引言

电流传送器 (Current conveyor 简记为 CC) 作为电流输出型有源器件在电路与系统中获得了广泛的应用, 它可以简化电路结构、降低器件功耗、扩展工作频带, 并具有很强的通用性和灵活性。利用电流传送器综合成的 n 阶有源滤波器具有功耗低、幅频特性好等特点, 具有很广阔的使用价值。本文研究了利用第二代电流传送器 (CCII) 和多端输出电流传送器 (MOCC) 综合生成 n 阶有源滤波器的方法。

### 2. 电流传送器

**2.1 CCII 电路结构** 电流传送器是 60 年代末期出现的一种集成器件, CCII 是第二代产品, 具有通频带宽、精度高、用途广等优点, 其电路符号如图 1 所示, 图中的+或-表示 CCII+或 CCII-, 数学描述为:

$$\begin{bmatrix} i_y \\ v_x \\ i_z \end{bmatrix} = \begin{bmatrix} 0 & 0 & 0 \\ 1 & 0 & 0 \\ 0 & 1 & 0 \end{bmatrix} \begin{bmatrix} v_y \\ i_x \\ v_z \end{bmatrix} \quad (1)$$

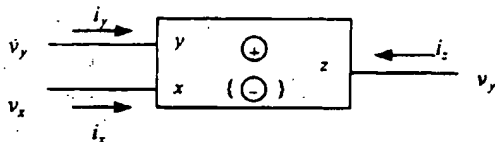


图 1 CCII 电路符号

**2.2 MOCC 电路结构** MOCC 是多输出端电流传送器, 其电路符号如图 2 所示, 它具有正输出端 Z 和负输出端 Z, 端口特性描述为:

$$\begin{bmatrix} i_y \\ V_x \\ i_{z1} \\ \vdots \\ i_{zm} \\ i'_{z1} \\ \vdots \\ i'_{zm} \end{bmatrix} = \begin{bmatrix} 0 & 0 & 0 & 0 \\ 1 & 0 & 0 & 0 \\ 0 & 1 & 0 & 0 \\ \vdots & \vdots & \vdots & \vdots \\ 0 & 1 & 0 & 0 \\ 0 & -1 & 0 & 0 \\ \vdots & \vdots & \vdots & \vdots \\ 0 & -1 & 0 & 0 \end{bmatrix} \begin{bmatrix} V_y \\ i_x \\ V_z \\ V'_z \end{bmatrix} \quad (2)$$

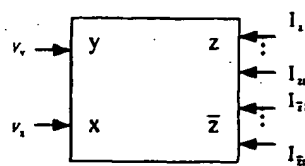


图 2 MOCC 电路符号

### 3. 用 CCII 实现 n 阶滤波器

n 阶滤波器电压传输函数为

$$H(s) = \frac{a_n s^n + a_{n-1} s^{n-1} + \dots + a_1 s + a_0}{s^n + b_{n-1} s^{n-1} + \dots + b_1 s + b_0} \quad (3)$$

相应的信号流程图如图 3 所示。根据此信号流图, 可以很容易地用 CCII 来实现 n 阶滤波器, 具体电路如图 4 所示。

由图 4 可以看出, 由 CCII 实现的 n 阶滤波器含有较多的元件, 为了尽量简化电路结构, 节省元件, 可采用 MOCC 来实现 n 阶滤波器。

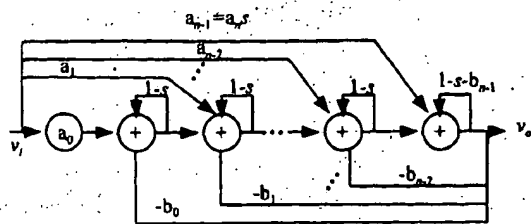


图3 式(3)对应的信号流图

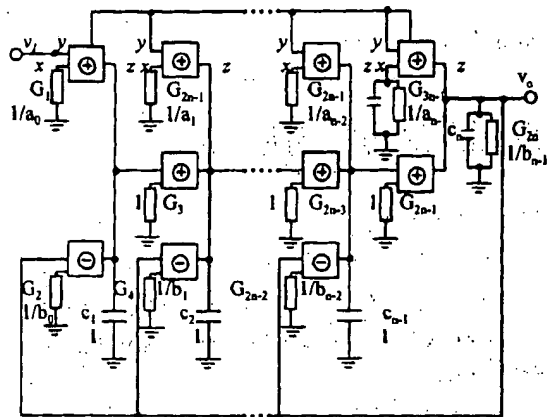


图4 用CCII实现的n阶滤波器

#### 4. 用MOCC实现n阶滤波器

由MOCC实现的n阶滤波器可以克服上述电路的不足, 本文以n阶高通滤波器为例介绍n阶滤波器的设计方法。n阶高通滤波器传输函数为

$$H(s) = \frac{as^n}{b_n s^n + b_{n-1} s^{n-1} + \dots + b_1 s + 1} \quad (4)$$

其信号流图如图5所示。图中 \$k\_j (j=0, 1, \dots, n)\$ 为输入传输比例因子, \$T\_i = 1/s\$ (\$\tau\_i\$ 为常数), 参数间关系为

$$\tau_n = b_1, \quad \tau_j = b_{n-j+1} \quad (j=n-1, n-2, \dots, 1)$$

$$k_0 = a/b_n, \quad k_n = -k_0 b_1 b_{n-1} / b_n$$

$$k_1 = -k_0 - \sum_{i=0}^{n-2} k_{n-i}$$

$$k_j = -\frac{b_{n-j}}{b_n} (k_0 b_{j-1} + \sum_{i=0}^{n-j-1} k_{n-i} b_{j+i} / b_{i+1})$$

$$(j=n-1, n-2, \dots, 2) \quad (5)$$

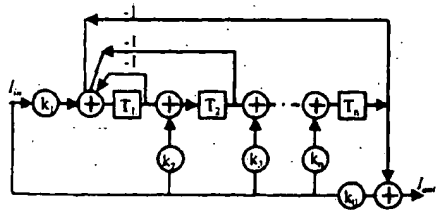


图5 式(4)对应的信号流图

根据图5用MOCC实现的电路如图6所示, 图中 \$R\_j C\_j = \tau\_j, R/R\_0 = k\_0\$。该电路只含有 \$n+1\$ 个MOCC, \$n\$ 个接地电容和 \$n+2\$ 个接地电阻, 与图3相比较, 大大减少了器件。

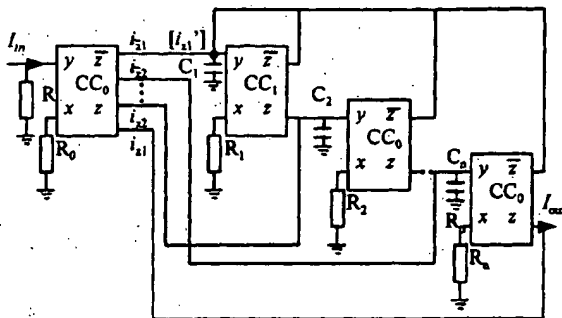


图6 用MOCC实现的n阶高通滤波器

#### 5. 设计举例

五阶巴特沃斯滤波器归一化传递函数为

$$H(s) = \frac{s^5}{s^5 + 3.236s^4 + 5.236s^3 + 5.236s^2 + 3.236s + 1}$$

根据式(5)可求出以下参数:

$$k_0=1, k_1=-5.003, k_2=4.004, k_3=-6.473, k_4=16.944, k_5=-10.472, \tau_1=0.309, \tau_2=0.618, \tau_3=1, \tau_4=1.618, \tau_5=3.236.$$

实现此五阶滤波器的电路含有6个MOCC, 其中 \$CC\_0\$ 输出 \$Z\$ 端有3个输出分支 \$i\_{z1}, i\_{z2}, i\_{z3}\$, 分别注入 \$I\_{out}, C\_2, C\_4\$, \$CC\_0\$ 输出 \$Z\$ 端有3个输出分支 \$i\_{z1}', i\_{z2}', i\_{z3}'\$ 分别注入 \$C\_1, C\_3, C\_5\$。电路图可参见图6, 电路参数分别为: \$R\_1=1k\Omega, R\_2=2.4k\Omega, R\_3=2.7k\Omega, R\_4=3.3k\Omega, R\_5=5.4k\Omega, C\_1=309pF, C\_2=257pF, C\_3=370pF, C\_4=490pF, C\_5=599pF\$。

#### 6. 结论

本文研究了用电流传送器实现n阶滤波器的设计方法, 其中用CCII实现的滤波器含有的元件较多, 而采用MOCC设计的n阶滤波器克服了其不足之处, 本文通过实例综合了5阶高通滤波器。由于该电路结构简单, 含有的元件少, 且功耗低、频带宽, 因而在信息处理电路中有很好的使用前景。

#### 参考文献

1. Chang C, Lee M S. Universal voltage-meas filter with three inputs and one output using three current conveyors and one voltage follower. Electronics Letters, 1994, 30(25), p2111-2113.
2. 何怡刚, 一种新颖的电流模式高通滤波器, 电工技术学报, 1999, vol. (14) 1, p55-58.



# IEEE Xplore®

RELEASE 1.8

Welcome  
United States Patent and Trademark Office

IEEE Xplore®  
1 Million Documents  
1 Million Users

[Help](#) [FAQ](#) [Terms](#) [IEEE Peer Review](#)
[Quick Links](#)
[» ABSTRACT PLUS](#)

Welcome to IEEE Xplore®

- ☐ Home
- ☐ What Can I Access?
- ☐ Log-out

Tables of Contents

- ☐ Journals & Magazines
- ☐ Conference Proceedings
- ☐ Standards

Search

- ☐ By Author
- ☐ Basic
- ☐ Advanced
- ☐ CrossRef

Member Services

- ☐ Join IEEE
- ☐ Establish IEEE Web Account
- ☐ Access the IEEE Member Digital Library

IEEE Enterprise

- ☐ Access the IEEE Enterprise File Cabinet

Print Format

[Search Results](#) [PDF FULL-TEXT 607 KB] [PREV](#) [NEXT](#) [DOWNLOAD CITATION](#)

## Low voltage, low power, high performance current mirror for portable analogue and mixed mode applications

Rajput, S.S. Jamuar, S.S.

Dept. of Electr. Eng., Indian Inst. of Technol., New Delhi

*This paper appears in: Circuits, Devices and Systems, IEE Proceedings [see also IEE Proceedings G- Circuits, Devices and Systems]*

Publication Date: Oct. 2001

On page(s): 273 - 278

Volume: 148, Issue: 5

ISSN: 1350-2409

Reference Cited: 7

CODEN: ICDSE7

Inspec Accession Number: 7093898

### Abstract:

A novel current mirror (CM), suitable for operation at low voltage levels is presented. The mirror has high input and high output voltage swings. Adaptive current biasing is introduced for minimising the effects of offset current. A compensation technique has been used to increase the bandwidth. This makes the CM structure attractive for portable, high frequency circuit applications. P-Spice simulations, based on models for 1.2  $\mu\text{m}$  technology, validate the operation of the proposed current mirror for currents from 1 to 500  $\mu\text{A}$  with 1.2 GHz bandwidth

### Index Terms:

CMOS analogue integrated circuits VLSI compensation current mirrors low-power electronics mixed analogue-digital integrated circuits 1 to 500  $\mu\text{A}$  1.2 GHz 1.2 micron HF circuit applications LV operation P-Spice simulations adaptive current biasing bandwidth compensation technique high frequency circuit applications high input voltage swing high output voltage swing high performance current mirror low power current mirror low voltage current mirror offset current portable analogue applications portable mixed mode applications

### Documents that cite this document

Select link to view other documents in the database that cite this one.

[Search Results](#) [PDF FULL-TEXT 607 KB] [PREV](#) [NEXT](#) [DOWNLOAD CITATION](#)

# Low voltage, low power, high performance current mirror for portable analogue and mixed mode applications

S.S. Rajput and S.S. Jamuar

**Abstract:** A novel current mirror (CM), suitable for operation at low voltage levels is presented. The mirror has high input and high output voltage swings. Adaptive current biasing is introduced for minimising the effects of offset current. A compensation technique has been used to increase the bandwidth. This makes the CM structure attractive for portable, high frequency circuit applications. P-SPICE simulations, based on models for 1.2 $\mu$ m technology, validate the operation of the proposed current mirror for currents from 1 to 500 $\mu$ A with 1.2GHz bandwidth.

## 1 Introduction

The demand for portability has made low power usage a key factor in integrated circuit design. Low power circuits normally find use in both digital and analogue mobile systems. Non-mobile applications also prefer to have low voltage (LV) operation to eliminate instrument-cooling requirements.

A CM is a common building block both in analogue and mixed mode VLSI circuits. Almost all high impedance CMs reported so far [1–3] need high input voltages, which give them the capability of high output voltage signal swing. The input voltage requirement for these CMs depends solely on the threshold voltage ( $V_t$ ) of the input MOSFET, thus making them unsuitable for low voltage operation. New low voltage CM (LVCM) circuits, therefore, need to be investigated for getting high signal swings at input and output terminals. A few CM topologies with reduced input voltage requirements have been reported in [4, 5], where either a level shifter or a bulk-driven approach [1] has been used. The CM proposed in [4] is capable of operating at a low supply of 1.3V, but it has limited current range (< 150 $\mu$ A) with a bandwidth of 100MHz. The CM proposed in [1] has limited current range (< 100 $\mu$ A), while that proposed in [5] is not suitable for high frequency applications.

A novel LVCM with adaptive biasing and high input and high output voltage swings is presented in this paper. Adaptive biasing enhances the input signal swing capability and reduces the undesirable offset current. The use of capacitive and resistive compensation gives a bandwidth of 1.2GHz. The proposed LVCM can operate at a bias voltage less than 1.2V for an input current less than 200 $\mu$ A;

and less than 1.7V for input current ranging from 200 to 500 $\mu$ A with output impedance of approximately 1M $\Omega$ .

## 2 LVCM topology

The simple CM topology shown in Fig. 1a requires input voltage ( $V_{in}$ ) of at least one  $V_t$ , and is unsuitable for any LV applications. The modified CM (Fig. 1b), which operates at low voltage, incorporates a level shifter PMOS transistor M4 (biased through a current  $I_{bias1}$ ) at input port. For this structure, we have

$$V_{ds1} = V_{gs1} - V_{gs4} \quad (1)$$

where  $V_{ds1}$  and  $V_{gs1}$  are the drain to source and gate to source voltages for M1.  $V_{gs4}$  is the gate to source voltage for M4.

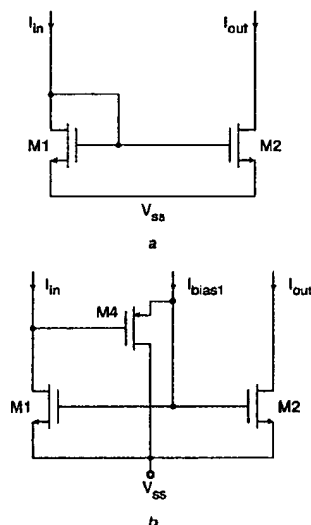


**Fig. 1** CM structures  
a Conventional CM structure  
b Conventional level shifted CM structure

M4 is operated in sub-threshold region and  $V_{gs4}$  is approximately 0.6 V. It is required to have a minimum  $V_{gs1}$  equal to at least one  $V_t$  to operate M1 in either linear/

© IEE, 2001

IEE Proceedings online no. 20010441

DOI: 10.1049/p-ods:20010441

Paper first received 20th September 2000 and in revised form 29th March 2001  
S.S. Rajput was with the Indian Institute of Technology and is now with the Thin Film Technology Group, National Physical Laboratory, Dr K.S. Krishnan Road, New Delhi, 110012, India

S.S. Jamuar is with the Department of Electrical Engineering, Indian Institute of Technology, Hauz Khas, New Delhi, 110016, India

saturation region. If  $V_{ds1}$  equals 0.2V, then M1 operates in the saturation region. However, M4 operates in the sub-threshold region for the entire input current ( $I_{in}$ ) range. The operation of M1 and M2 depends on  $I_{in}$  and their aspect ratios ( $W/L$ ). Hence, when  $I_{in} < 1.0\mu A$ , M1 operates in the sub-threshold region and when  $I_{in}$  exceeds  $1.0\mu A$ , M1 operates in the saturation region.

### 2.1 Operation in sub-threshold region

At low input currents, M1 and M2 operate in the sub-threshold regions and the input voltage present due to the injection of  $I_{in}$  is given by

$$V_{in} \approx \eta V_T \left[ \log \frac{I_{DO4} L_1 W_4}{I_{DO1} L_4 W_1} \frac{I_{in}}{I_{bias1}} \right] \quad (2)$$

where  $V_T$  is the thermal voltage.  $I_{DO1}$  and  $I_{DO4}$  are process parameters, ( $W/L$ ) represents transistor aspect ratio, and  $\eta$  lies between 1.2 and 2.0.

As  $I_{in}$  increases, both M1 and M2 enter into the saturation region and the circuit analysis carried out in the following Sections assumes that M1 and M2 are in the saturation regions.

### 2.2 Proposed LVCM structure

The CM structures shown in Fig. 1 do not have high output resistance. The LVCM structure shown in Fig. 2 is based on the triode transconductor structure [6], and is expected to increase the output resistance. The input current  $I_{in}$  is pumped into the drain of M1. The bias current of M4 is kept small so that M4 operates in the sub-threshold region and M1 is in the saturation region. The transconductance ( $g_{m1}$ ) and channel conductance ( $g_{d1}$ ) of M1 decide the input impedance ( $R_{in}$ ). Here, M4 provides the requisite gate bias for M1 and M2 while M5 provides suitable bias for M3.  $V_{in}$  is given by

$$V_{in} = \sqrt{\frac{2I_{in}}{\beta_1}} + \Delta V_{th} - \left| \eta V_T \ln \left( \frac{L_4 I_{bias1}}{W_4 I_{DO4}} \right) \right| \quad (3)$$

where  $\Delta V_{th}$  ( $= V_{tp} - V_{tn}$ ) is the mismatch between the threshold voltages of M1 and M4 and  $\beta_1$  represents the transconductance parameter for M1.

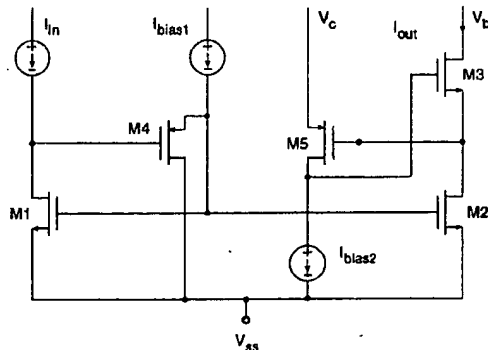


Fig. 2 Proposed high output impedance LVCM

$V_{gs1}$  and  $V_{gs2}$  are equal, but  $V_{ds2}$  depends on the applied bias voltage ( $V_B$ ), output current ( $I_{out}$ ) and the bias current of M5 ( $I_{bias2}$ ). We choose  $I_{bias2}$  to be  $10\mu A$ , which ensures that M5 operates in the linear region for entire range of  $V_B$  because the drain gate voltage of M5 equals  $V_{gs3}$ .

For a current flow through M3 and M2, lower  $V_B$  implies lower  $V_{ds2}$ . This causes higher  $V_{gs5}$  than that required for  $I_{bias2}$  to flow.  $V_{ds5}$  depends on the gate bias of M3 and is at least equal to  $V_{ds2} + V_{in}$ . These conditions

ensure that M5 operates in the linear region. Also,  $V_{ds2}$  increases as  $V_B$  is increased and M3 has to pump  $I_{out}$  but drain source voltage of M3 is small and inadequate for the purpose. Hence, it requires higher gate source bias, which equals the difference of applied voltage at source of M5 ( $V_C$ ) and the drain voltage of M2 ( $= V_C - V_{ds5}$ ).  $V_C$  is normally taken as  $V_{DD}$  itself. Now,  $V_B$  divides between  $V_{ds2}$  and  $V_{ds3}$  as:

$$\frac{V_{ds2}}{V_{ds3}} = \frac{\beta_3(V_C - V_{ds2} - V_{tn})}{\beta_2(V_{ds1} + V_{gs4} - V_{tp})} \quad (4)$$

When  $V_B$  is small, the above ratio is high and  $V_{ds2}$  equals  $V_B$ . With the increase in  $V_B$ ,  $V_{ds2}$  rises as M5 enters into the saturation from the linear region. When  $V_{ds2}$  increases further,  $V_{gs3}$  decreases to a minimum value where further decrease in  $V_{gs3}$  will not allow  $I_{out}$  to flow. Now the increase in  $V_{ds2}$  stops and remains fairly independent and  $V_{ds3}$  starts rising. M3 enters into saturation, resulting M5 to be always in the linear region.

The input impedance ( $R_{in}$ ) and the output impedance ( $R_{out}$ ) are given by

$$R_{in} \approx \frac{1}{g_{m1}} \quad (5)$$

$$R_{out} \approx \frac{g_{m3}}{g_{d2}g_{d3}} \quad (6)$$

where  $g_{d2}$  and  $g_{d3}$  represent the output conductances of M2 and M3, while  $g_{m1}$  and  $g_{m3}$  represent transconductances of M1 and M3, respectively. Similarly, the minimum output voltage necessary for CM operation is equal to:

$$V_{out}(\min) = V_{ds2}(\min) + V_{ds3}(\min) \quad (7)$$

### 3 Adaptive biasing technique

For the LVCM of Fig. 2, a minimum  $I_{bias1}$  is required and  $V_{in}$  is dependent of both  $I_{in}$  and  $I_{bias1}$ . If  $I_{in}$  is increased, then  $V_{in}$  also increases. But this increase can be reduced to a smaller value by increasing  $I_{bias1}$ . It is possible to increase  $I_{bias1}$  proportional to  $I_{in}$  by using the CMs obtained using M6, M7 and M8 (Fig. 3). The current through M8 is proportional to  $I_{in}$  and is  $I_{bias1}$ .

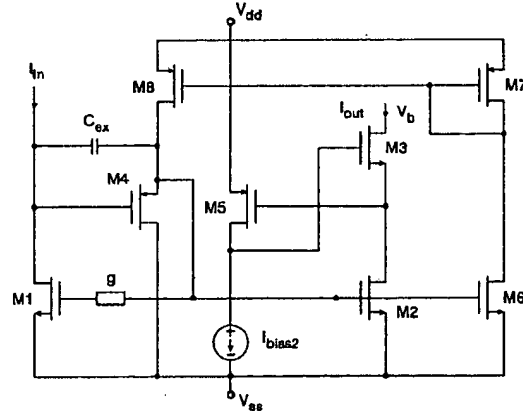


Fig. 3 Proposed ABLVCM structure

The gate source voltage for M2 ( $V_{gs2}$ ) is given by

$$V_{gs2} = V_{ds1} + \left| \eta V_T \ln \left( \frac{L_4 I_{bias1}}{W_4 I_{DO4}} \right) \right| + |V_{tp4}| \quad (8)$$

where  $V_{tp4}$  is the threshold voltage of M4.

We find that  $V_{gs2}$  depends on  $V_{th1}$  and  $I_{bias1}$ . For low input current ( $I_{in} \leq 1 \mu A$ ),  $V_{ds2}$  is nearly equal to zero volts and  $I_{bias1}$  solely decides  $V_{gs2}$ .  $I_{bias1}$  drives  $V_{gs2}$  to be near  $V_{in}$  even for zero  $I_{in}$ .  $V_{in}$  will also be zero, but  $V_{ds2}$  increases independently with  $V_B$ . Under this condition, a current flows through M2 (even though  $I_{in}$  is zero), because  $I_{bias1}$  decides the gate bias for M2 and  $V_{ds2}$  increases independently with  $V_B$ . This condition drives M2 into the sub-threshold region and a small current, known as the offset current ( $I_{offset}$ ), flows through M2. As  $I_{bias1}$  increases, the gate source bias of M2 increases, although  $V_{in}$  is still negligible ( $\approx 0.0 V$  for  $I_{in} < 1 \mu A$ ). This causes  $I_{offset}$  to increase. Thus,  $I_{offset}$  restricts the increase in  $I_{bias1}$ .

Thus two contradictory requirements emerge (i.e. that  $I_{bias1}$  should be increased to keep  $V_{in}$  low and at the same time  $I_{bias1}$  should be decreased to keep  $I_{offset}$  low). In the design of an adaptively biased LVCM (ABLVCM),  $I_{bias1}$  is kept low, when  $I_{in}$  is low and is increased for higher  $I_{in}$ . Higher  $I_{bias1}$  imparts low  $V_{in}$  at higher  $I_{in}$  and lower  $I_{bias1}$  is necessary at low  $I_{in}$  to have low  $I_{offset}$ . Fig. 4 gives the values of offset current under different operating conditions.

We find that  $I_{offset}$  can also be minimised by matching the threshold voltages of the PMOS and NMOS transistors, but cannot be made zero. As shown in Fig. 4, operation of the PMOS transistor in the sub-threshold region reduces  $I_{offset}$  by a factor of 3. We have used this concept in the proposed ABLVCM structure.

#### 4 Circuit modelling

The goal of circuit modelling is to obtain the functional relationship among the input and output variables, which depends upon some physical and bias parameters. Hybrid ( $h$ ) parameters to model the small-signal behaviour for the LVCM are given in Fig. 5, where

$$C_{in} = C_{gd4} + C_{gs1} + C_{gd1} - \frac{g_{d4}(C_{gs4} + C_{gd1} + C_{ex})}{g_{m4}} \quad (9)$$

$$g_l = g + g \frac{C_{gs1}}{C_{gd1}} + g_{gd2} \quad (10)$$

$$C_p \approx C_{gs1} + C_{gs2} + C_{gs4} + C_{gd1} \quad (11)$$

$$C_x \approx C_p + C_{ex} \quad (12)$$

and  $g$  is the conductance connected between gates of M1 and M2.

#### 5 Frequency enhancement

The high frequency response of the LVCM is described by the parameter  $h_{21}$  (Fig. 5). The addition of an external capacitor  $C_{ex}$  between the gate and source of M4 decreases the input capacitance  $C_{in}$  (eqn. 9) and increases  $C_x$  (eqn. 12). This results in shifting the pole-location away from the imaginary axis in the complex plane and the bandwidth decreases. But addition of  $g$ , as proposed in [7],

Parameter	Operating conditions	
	M1, M2, and M4 (in sub-threshold)	M1 and M2 (in sub-threshold) and M4 (in saturation)
$I_{offset}$	$\frac{W_2}{L_2} \frac{L_4}{W_4} \frac{I_{DO2}}{I_{DO4}} I_{bias1} \exp\left(\frac{\Delta V_{th}}{\eta V_T}\right)$	$\frac{\beta_2}{2} \left\{ \sqrt{\frac{2I_{bias1}}{\beta_4}} + \Delta V_{th} \right\}^2$
$I_{offset}$ (Minimum)	$\frac{W_2}{L_2} \frac{L_4}{W_4} I_{bias1}$	$\frac{K_2}{K_4} \frac{W_2}{L_2} \frac{L_4}{W_4} I_{bias1}$

Fig. 4  $I_{offset}$  under different operating conditions

hybrid ( $h$ ) parameters	Low frequency	High frequency
$h_{11}$	$\frac{g_{d4}}{g_{m1}g_{m4} + g_{d1}g_{d4}}$	$\frac{1}{g_{d1} + sC_{in}}$
$h_{12}$	0	0
$h_{21}$	$\frac{g_{m2}}{g_{m1}}$	$\frac{g_{m2}(g_l + g_{m4} + sC_x)}{(g_{d1} + sC_m)(g_l + sC_x)}$
$h_{22}$	$\frac{g_{d2}g_{d3}}{g_{d2} + g_{d3}}$	$\frac{g_{d2}g_{d3} \left(1 + \frac{sC_{gd5}}{g_{d2}}\right) \left(1 + \frac{sC_{gs5}}{g_{d3}}\right)}{(g_{d2} + g_{d3}) \left(1 + \frac{s(C_{gd5} + C_{gs5})}{g_{d2} + g_{d3}}\right)}$

Fig. 5 Hybrid ( $h$ ) parameters

increases  $g_t$ . This compensates for increase in  $C_x$ . When  $g_t \gg g_{m4}$ ,  $h_{21}$  reduces to following:

$$h_{21} \approx \frac{g_{m2}}{g_{d1} + sC_{in}} \quad (13)$$

We find that  $C_{in}$  primarily decides the bandwidth of ABLVCM if  $g_{d1}$  is constant. Reducing  $C_{in}$  can increase the bandwidth of ABLVCM. This is achieved by addition of the external capacitance  $C_{ex}$ .

## 6 Sensitivity analysis

Sensitivity analysis of the CM is carried out to find the variation of the output current ( $I_{out}$ ) for the variations in various critical device parameters.  $I_{out}$  is given by

$$I_{out} = \frac{\mu C_{OX} W}{2L} \times \left[ V_{ds1} + \left| \eta V_T \ln \left( \frac{L_4}{W_4} \frac{I_{bias1}}{I_{DO4}} \right) \right| + |V_{tF4}| - V_{tn2} \right]^2 \quad (14)$$

The sensitivity of  $I_{out}$  was evaluated with respect to various parameters. The following observations are made from the sensitivity calculations.

For  $V_{ds2}$  less than 2.0V, the sensitivity of the output current to  $V_{ds2}$  change is almost negligible. Any variations occurring in the transistor dimensions ( $W$  and  $L$ ) have immediate reflection on  $I_{out}$ . The sensitivity of  $I_{out}$  to  $I_{bias1}$  change is almost negligible and the sensitivity of  $I_{out}$  to the threshold voltage change is quite high, as is expected from any CM structure.

To calculate sensitivity of  $I_{out}$  to  $I_{in}$ , we assume  $K_1 = K - \Delta K$ ,  $K_2 = K + \Delta K$ ,  $V_{t1} = V_t - \Delta V_t$  and  $V_{t2} = V_t + \Delta V_t$ . The current  $I_{out}$  is given by

$$I_{out} = \frac{\beta_2}{2} \left( \sqrt{\frac{2I_{in}}{\beta_1}} - 2\Delta V_t \right)^2 \quad (15)$$

For  $\beta_1 = \beta_2$  we get

$$S_{I_{in}}^{I_{out}} \approx 1 - \frac{\Delta K}{K} \quad (16)$$

and the sensitivity of  $I_{out}$  to  $I_{in}$  is dependent on variation in  $K$ .

## 7 Temperature dependence

Several of MOSFET parameters such as mobility ( $\mu$ ) and the threshold voltage ( $V_t$ ) are temperature dependent and their effects on CM performance need to be evaluated. For the ABLVCM under consideration,  $I_{out}$  is given by

$$I_{out} = \mu(T_0) T^{-3/2} \frac{C_{OX} W_2}{2L_2} \times \left[ V_{ds1} + \frac{nkT}{q} \ln \left( \frac{L_4}{W_4} \frac{I_{bias1}}{I_{DO4}} \right) + \Delta V_{th} \right]^2 \quad (17)$$

Assuming the temperature changes in  $\Delta V_{th}$  to be zero, the fractional temperature coefficient ( $TC_f$ ) is given as

$$TC_f(I_{out}) = \frac{-1.5}{T} + \frac{2K_2 \frac{nk}{q} \frac{W_2}{L_2} \ln \left( \frac{L_4}{W_4} \frac{I_{bias1}}{I_{DO4}} \right)}{g_{m2}} \quad (18)$$

where  $K_2 = \mu C_{OX}$  for M2. ABLVCM can be made temperature insensitive by selecting various parameters. If  $(L_4/W_4)$  is small and  $I_{DO4} \gg I_{bias1}$ , we have

$$TC_f(I_{out}) = \frac{-1.5}{T} \quad (19)$$

This gives quite low  $TC_f(I_{out})$ , equal to 500ppm/°C at room temperature.

## 8 Simulation results

The parameters such as  $R_{in}$ ,  $R_{out}$ , bandwidth and  $I_{offset}$ , which should be bias insensitive, decide the performance of the ABLVCM. The CM should also have high input and output voltage swing capabilities. The circuits have been simulated using level 3 SPICE parameters for 1.2μm technology with supply voltage of ±1V. The ( $W/L$ ) ratios for various MOSFETS are given in Table 1.

Table 1: Aspect ratios

Device number	Type	Aspect ratio ( $W \mu m / L \mu m$ )	Figure number(s)
M1, M2	NMOS	84/2.4	2, 3
M3	NMOS	60/1.2	2, 3
M4, M5	PMOS	18/1.2	2, 3
M6	NMOS	8.4/2.4	3
M7	PMOS	120/1.2	3
M8	PMOS	2.4/4.8	3

### 8.1 LVCM

P-SPICE simulations were carried out for  $I_{bias1}$  and  $I_{bias2}$  of 100pA and 10μA respectively, for  $I_{in}$  between 1μA and 500μA. Input voltage ( $V_{in}$ ) is plotted in Fig. 6 for various values of  $I_{in}$ .  $V_{in}$  required is 0.8V as against 1.36V for conventional CM for 500μA of  $I_{out}$ . This voltage is still higher for low voltage CM applications. For  $I_{out} < 200\mu A$ , the circuit operates with  $V_{in} < 0.5V$ . The variation of  $V_{in}$  as

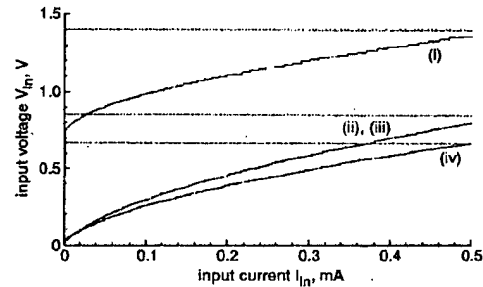


Fig. 6  $V_{in}$  against  $I_{in}$  characteristics (i) Conventional CM; (ii) simple CM structure; (iii) proposed LVCM structure; (iv) proposed ABLVCM

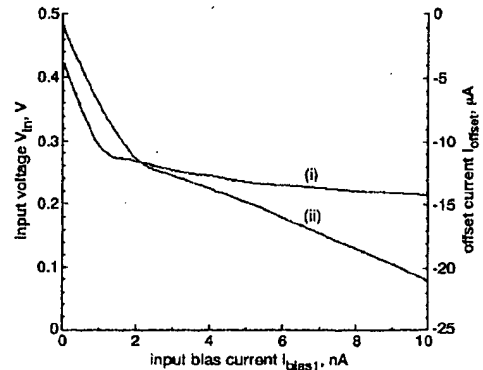


Fig. 7  $V_{in}$  developed at the input port for  $I_{in} = 100\mu A$  and  $I_{offset}$  characteristics as a function of  $I_{bias1}$  (i) Input voltage ( $V_{in}$ ); (ii) offset current ( $I_{offset}$ )



a function of  $I_{bias1}$  is shown in Fig. 7 for  $I_{in}$  of 100  $\mu$ A (trace (i)). Variation of  $I_{offset}$  as a function of  $I_{bias1}$  is also shown (trace (ii)). There is an  $I_{offset}$  of 5  $\mu$ A for  $I_{bias1}$  of 1 nA and any decrease in  $I_{bias1}$  needs a higher  $V_{in}$  with reduced  $I_{offset}$ .  $I_{out}$  as a function of  $V_D$  for different values of  $I_{in}$  is given in Fig. 8, where  $I_{offset}$  is visible, when  $I_{in}$  is less than 10  $\mu$ A (inset of Fig. 8).

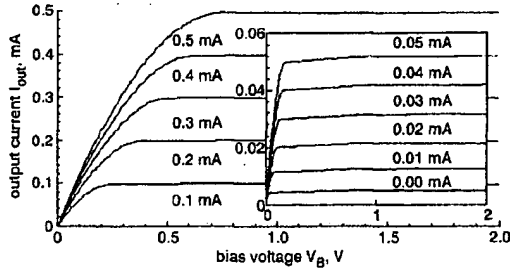


Fig. 8 Current-voltage characteristics for proposed LVCM  
Figure in inset shows I-V characteristics at low currents

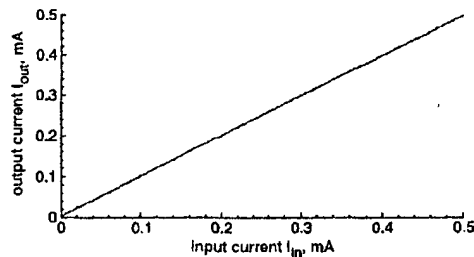


Fig. 9 Current transfer characteristics of proposed LVCM

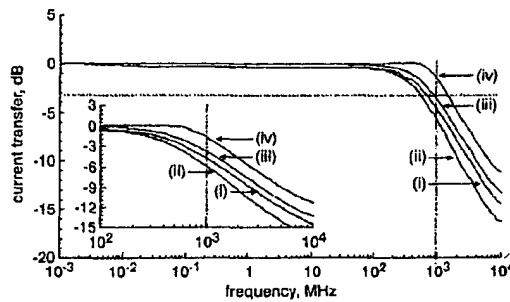


Fig. 10 Frequency response of proposed LVCM  
(i) Without compensation; (ii) with resistive compensation; (iii) with capacitive compensation; (iv) with resistive and capacitive compensation  
Figure shown in the inset depicts the expanded characteristics near cutoff frequency

We find that  $I_{out}$  to  $I_{in}$  ratio is almost equal to 1 (Fig. 9). The bandwidth is strongly dependent on the type of compensation used (as in Fig. 10 for  $I_{in}$  of 500  $\mu$ A). The bandwidth is about 630 MHz (trace (i)) with no compensation. With addition of gate resistance, bandwidth reduces to approximately 500 MHz (trace (ii)). There is a sag in the frequency response around 10 kHz due to the presence of a zero around this frequency. Compensating capacitor increases the bandwidth to 790 MHz (trace (iii)). With both external capacitor and resistance, the bandwidth increases twofold to 1.2 GHz (trace (iv)) and the sag also disappears due to cancellation of zero by the addition of pole. The corresponding bandwidth for conventional CMs was found to be 550 MHz (Fig. 1a), and 382 MHz (Fig. 1b) and sag was also present.

## 8.2 ABLVCM

The ABLVCM uses adaptive biasing and frequency enhancement techniques.  $R_{in}$  and  $R_{out}$  are found to be

1.8 k $\Omega$  and 1 M $\Omega$ , respectively, at a supply voltage of  $\pm 1$  V. The sensitivity analysis of  $I_{out}$  with respect to the changes in the bias currents and bias voltages indicates that the variations in  $I_{out}$  are negligible.

The  $I_{in}$  against  $V_{in}$  characteristics for ABLVCM is also shown in Fig. 6. We find that  $V_{in}$  is 0.65 V for  $I_{in}$  of 500  $\mu$ A, whereas it was 0.8 V and 1.36 V for the LVCM and the conventional CM, respectively. Fig. 11 is the plot of bias voltage against  $I_{out}$  for different values of  $I_{in}$ .  $I_{offset}$  is less than 1  $\mu$ A (inset of Fig. 11). It requires an output voltage less than 0.4 V for  $I_{in}$  up to 200  $\mu$ A and approximately 0.65 V for  $I_{in}$  up to 500  $\mu$ A.

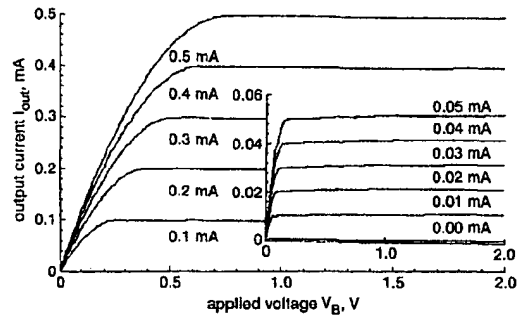


Fig. 11 Current-voltage characteristics for proposed ABLVCM  
Figure in the inset shows I-V characteristics at low currents

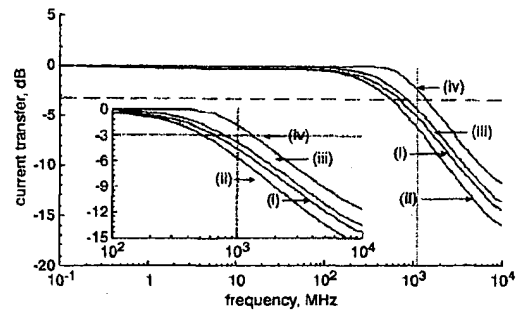


Fig. 12 Frequency response of proposed ABLVCM  
(i) Without compensation; (ii) with resistive compensation; (iii) with capacitive compensation; (iv) with resistive and capacitive compensation  
Figure shown in the inset shows the expanded characteristics near cutoff frequency

The frequency response of ABLVCM is similar to that of the LVCM and the bandwidth is dependent on the type of compensation used (Fig. 12). The bandwidth with and without compensation is the same as in the LVCM. Simulations show that the bandwidth was 90 MHz, 150 MHz, and 210 MHz for ABLVCM; 95 MHz, 150 MHz, and 200 MHz for the CM of Fig. 1a; and 2 kHz, 115 MHz, and 140 MHz for the CM of Fig. 1b, respectively, when  $I_{in}$  equals 10  $\mu$ A, 30  $\mu$ A and 50  $\mu$ A, respectively.

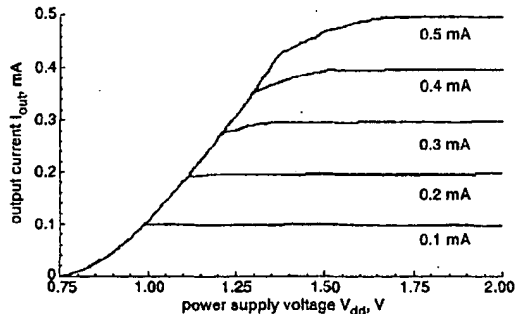


Fig. 13 Bias requirement for ABLVCM

Simulations were also carried out under different supply voltages to define the bias requirements (Fig. 13). For currents less than  $400\mu\text{A}$ , the circuit performs satisfactorily at a single supply of  $1.5\text{V}$ . However, bias voltage of more than  $1.6\text{V}$  is needed for  $I_{in}$  more than  $400\mu\text{A}$ .

The bandwidth of the proposed circuit was evaluated by simulating it at different voltage levels from  $\pm 0.625\text{V}$  to  $\pm 1.0\text{V}$  at  $I_{in}$  of  $200\mu\text{A}$ . The bandwidth of the ABLVCM was independent of bias voltage when the latter is more than  $\pm 0.75\text{V}$  and was approximately  $790\text{MHz}$ . However for voltages less than  $\pm 0.75\text{V}$ , the bandwidth falls to  $620\text{MHz}$  at  $\pm 0.625\text{V}$ . Worst-case analysis was carried out to find variations in  $I_{out}$  for 50% Gaussian deviations in the model parameters chosen for MOSFETs. The absolute error present in the DC current transfer is almost negligible for changes in model parameters ( $3\mu\text{A}$  at  $120\mu\text{A}$ ). The error in AC current transfer is also negligible. The bandwidth of the ABLVCM decreases by 5% over a temperature change from  $0$  to  $100^\circ\text{C}$ .

### 8.3 Comparative performance

We observe that the ABLVCM has better performance than other circuits. It operates satisfactorily with input voltage as low as  $0.65\text{V}$  for current up to  $500\mu\text{A}$ , whereas the other LVCM require more than  $0.8\text{V}$  (Figs. 6, 8 and 11). It has quite low offset current. A supply voltage of  $1.5\text{V}$  is needed to ensure proper bias requirement for M4 and M5; but other structures require higher voltage.

## 9 Conclusion

A novel high performance CMOS LVCM, which can operate with a supply voltage of  $1.5\text{V}$ , is presented. The ABLVCM has wide input current range  $1\mu\text{A}$  to  $400\mu\text{A}$  at

$1.5\text{V}$  with rail-to-rail input and output voltage swing. At  $2\text{V}$ , the ABLVCM can operate up to  $500\mu\text{A}$ . It has high bandwidth of approximately  $1.2\text{GHz}$ . One immediate application is in the design of handheld equipment, where supply voltage and current are parameters of prime importance. This circuit can find wide-ranging applications in portable equipment, where analogue and mixed mode circuits are used.

## 10 Acknowledgment

S.S. Rajput thanks Dr. R. Bhattacharyya, Head, Thin Film Technology Group, NPL, New Delhi, for his keen interest in the work.

## 11 References

- 1 BLALOCK, B.J., ALLEN, P.E., and RINCON-MORA, G.A.R.: 'Designing 1-V Op Amps using standard digital CMOS technology', *IEEE Trans Circuits Syst. II, Analog. Digit. Signal Process.*, 1998, **45**, pp. 769-780
- 2 ZEKI, A., and KUNTMAN, H.: 'Accurate and high output impedance current mirrors suitable for CMOS current output stages', *Electron. Lett.*, 1997, **33**, pp. 1042-1043
- 3 MULDER, J., WOERD, A.C., SERDIJN, W.A., and ROERMUND, A.H.M.: 'High swing cascode MOS current mirror', *Electron. Lett.*, 1996, **32**, pp. 1251-1252
- 4 PRODANOV, V.I., and GREEN, M.M.: 'CMOS current mirrors with reduced input and output voltage requirements', *Electron. Lett.*, 1996, **32**, pp. 104-105
- 5 HEIM, P., and JABRI, M.: 'A MOS cascode-current mirror biasing circuit operating at any current level with minimal output saturation voltage', *Electron. Lett.*, 1995, **31**, pp. 690-691
- 6 LIKITTANAPONG, P., WORAPISHEET, A., and TOUMAZAU, C.: 'Linear CMOS triode trans conductor for low voltage applications', *Electron. Lett.*, 1998, **34**, pp. 1224-1225
- 7 VOO, T., and TOUMAZAU, C.: 'Precision temperature stabilized tunable CMOS current mirror for filter applications', *Electron. Lett.*, 1996, **32**, pp. 105-106